MITSUBISHI ELECTRIC RESEARCH LABORATORIES
https://www.merl.com

Fermi-Level Pinning Effect in Gate Region: A Case Study of Multi-Metal Gated AlGaN/GaN HEMT for High RF Linearity

Hossain, Toiyob; sikder, Bejoy; Azad, Md.Tasnim; Xie, Qingyun; Yuan, Mengyang; Yagyu, Eiji; Teo, Koon Hoo; Palacios, Tomas; Chowdhury, Nadim

TR2024-010 March 01, 2024

Abstract

This work investigates the robustness of AlGaN/GaN multi- metal gated (MMG) HEMT architecture for gm3 optimization and linearity improvement in the presence of Fermi-Level pinning. Through Technology Computer-Aided Design (TCAD), Compact modeling and Load-Pull simulations, it is shown that despite incorporating FLP, employing MMG scheme improves device level gm3-suppression leading to an improvement in OIP3/Pdc and IMD3. Remarkably, OIP3/Pdc of 18.9 dB is obtained considering an FLP factor of 0.43, which is 10.7 dB improvement than the conventional planar HEMT. A comparative analysis on output power back-off (OBO) for conventional and MMG HEMT with different FLP factors establishes MMG as a robust architecture to FLP, and therefore a practical method to enhance linearity of GaN power amplifiers.

IEEE Electron Devices Technology & Manufacturing Conference 2024

© 2024 IEEE. Personal use of this material is permitted. Permission from IEEE must be obtained for all other uses, in any current or future media, including reprinting/republishing this material for advertising or promotional purposes, creating new collective works, for resale or redistribution to servers or lists, or reuse of any copyrighted component of this work in other works.

Mitsubishi Electric Research Laboratories, Inc.
201 Broadway, Cambridge, Massachusetts 02139

Fermi-Level Pinning Effect in Gate Region: A Case Study of Multi-Metal Gated AlGaN/GaN HEMT for High RF Linearity

Toiyob Hossain[1], Bejoy Sikder[1], Md. Tasnim Azad[1], Qingyun Xie[2], Mengyang Yuan[2], Eiji Yagyu[3], Koon Hoo Teo[4], Tomás Palacios[2], and Nadim Chowdhury[1*]

[1]Bangladesh University of Engineering and Technology, Dhaka-1205, Bangladesh

[2]Massachusetts Institute of Technology, Cambridge, MA 02139, U.S.A.

[3]Mitsubishi Electric Corporation, Amagasaki 661-8661, Japan

[4]Mitsubishi Electric Research Laboratories, Cambridge, MA 02139, U.S.A.

* Email: nadim@eee.buet.ac.bd

Abstract

This work investigates the robustness of AlGaN/GaN multi-metal gated (MMG) HEMT architecture for g_{m3} optimization and linearity improvement in the presence of Fermi-Level pinning. Through Technology Computer-Aided Design (TCAD), Compact modeling and Load-Pull simulations, it is shown that despite incorporating FLP, employing MMG scheme improves device level g_{m3}-suppression leading to an improvement in OIP3/P_{dc} and IMD3. Remarkably, OIP3/P_{dc} of 18.9 dB is obtained considering an FLP factor of 0.43, which is 10.7 dB improvement than the conventional planar HEMT. A comparative analysis on output power back-off (OBO) for conventional and MMG HEMT with different FLP factors establishes MMG as a robust architecture to FLP, and therefore a practical method to enhance linearity of GaN power amplifiers.

Keywords: AlGaN/GaN HEMT, Fermi-Level Pinning, Linearity, Multimetal Gate

Introduction

To accommodate the surging demand of highly efficient linear amplifiers for 5G and beyond communication networks, GaN HEMT-based power amplifiers (PA) are emerging as the ideal candidates. Poised with the best in-class power-density and power-added-efficiency (PAE) **[1-2]**, GaN HEMT technology is a suitable candidate for the next generation base station PAs. However, due to a strong non-linearity observed at the high input power, GaN-based PAs are limited to operating at certain OBO which eventually limits the efficient operation of the same. Of the various factors at the device level that contribute to the nonlinearity of a signal in a PA, it is the third-order transconductance (g_{m3}) that exerts the most significant influence (48% contribution). **[3]**. Threshold voltage (V_t) engineering is an effective technique for the reduction of g_{m3} and hence the improvement of large-signal linearity performance **[4].**

Fermi-Level Pinning (FLP) is a practical problem faced by GaN HEMTs which depends highly on sample preparation, surface treatment, and post gate annealing **[5]**. However, despite several experimental reports on FLP, there is a lack-of studies to understand the device performance in the presence of FLP. Such a problem becomes more pronounced in a multi-metal gated (MMG) architecture **[6]**. MMG HEMT was recently reported for g_{m3} compensation, exhibiting a significant RF linearity improvement (6.3 dB higher OIP3/P_{dc}, 12.9 dB less IMD3 compared to conventional planar architecture with single metal-gate). In MMG scheme the modulation of V_t was achieved by placing different metals along the width of the device which led to lower g_{m3}. However, the proposed technique assumed an ideal Schottky behavior of the gate metals without considering FLP, a first order non-ideal effect of practical metal/semiconductor contacts. The problem of FLP becomes more pronounced in MMG HEMT where 10 metals are studied together for g_{m3} optimization through V_t modulation.

Using the case study of the recently proposed MMG AlGaN/GaN HEMT, this work establishes MMG as a robust architecture for improving GaN HEMT's linearity in the presence of FLP through a systematic investigation. Through TCAD simulation and large-signal assessment, this work not only validates the MMG scheme in the non-ideal practical scenarios, but also demonstrates that even in the presence of FLP, the alleviation of g_{m3} nonlinearity improves RF large-signal linearity metrics. In light of the experimentally reported FLP factor values, it is observed that all linearity metrics show improvements compared to a planar HEMT.

Device Structure and Simulation Methodology

The 3-D schematic of the proposed MMG is shown in Fig. 1(a). M_1, M_2 and M_3 are the representative metals which are placed along the width of the device to modulate V_t. Fundamentally, this technique follows the principle of parallel connected HEMTs each with distinct V_t to achieve a slow turn on and hence, lower values of the derivatives of transconductance. Fig. 1(b) shows a circuit-level ideation of the device, whose dimensions are given in Fig. 1(c). The simulation framework includes experimentally calibrated TCAD models, g_{m3} optimization, compact modeling, and finally large-signal simulation for performance evaluation of the PA, as reported in Fig. 1(d) **[7-8].** Key simulation parameters have been reported in **[6].**

The FLP effect has been considered in the simulation framework through the dependence of the threshold voltage for a HEMT on the Schottky barrier height (SBH) as given in Eq. (2). Ideally, V_t modulation should be exactly 1 V for a change of 1 eV in metal work-function (Φ_m), or in other words, a slope of S = 1 V/eV. However, FLP restricts the variation of SBH despite a variation in Φ_m and so using multiple metals in the gate of the device cannot change V_t indefinitely. In literature, in the presence of FLP, the dependence of SBH on Φ_m is described by a slope parameter S instead of ideal slope 1 V/eV. S = 1 implies the ideal case with no pinning and S = 0 indicates that the Fermi level is pinned at a certain energy level for all metals. Previous reports of metal/AlGaN contacts show S values of 0.84±0.26, and 0.43 [**9**]. In this work, two values (0.43 and 0.70) of S have been investigated to quantify the effect on g_{m3} improvement (and therefore RF linearity) in MMG HEMT.

Results and Discussion

Fig. 2(a) shows the variation of V_t with respect to Φ_m for different values of S. The standard deviation of threshold voltage is 0.55 V for S = 1, 0.38 V for S = 0.70 and 0.24 V for S = 0.43. As previously mentioned, MMG HEMT achieves the lower g_{m3} through the superposition of adjacent gate-metal's g_{m3}'s. Therefore, their V_t distribution is an important

factor for the degree of optimization. Fig. 2(b), (d) and (f) depict the g_{m3} profile for different FLP factors. The resulting decrease in the standard deviation of V_t leads to a narrower optimization window for g_{m3} cancellation. The metal work functions, and their gate-widths are chosen by employing the optimization technique explained in [**6**]. In [**6**], a 3× suppression of g_{m3} is achieved by an optimum choice of six metals for S = 1. It was found that, the optimized results benefit from the consideration of FLP. Notably, a 3.2× and 3.4× reduction in g_{m3} is achieved for S = 0.70 and 0.43 respectively [Fig. 2(e)-(g)] using only four metals (W-19.5%, Ru-14.9%, Ni-30.2%, Au-35.4% for S = 0.70, and W-18.7%, Ru-13.8%, Ni-23.7% Au-43.8% for S = 0.43). To explain, the metals chosen have work-functions which are relatively far apart, but FLP allows the g_{m3} curves to fall within a narrow optimization window. Thus, considering finite FLP leads to a better g_{m3} compensation which eventually results in a superior result with a smaller number of metals. Fig. 2(h) depicts the enhancement in optimization, as stated.

Nevertheless, it may seem that a greater extent of FLP would result in better g_{m3} suppression and enhanced linearity, which is not the case. A complete FLP might cause the peaks of g_{m3} for certain metals to overlap, reinforcing g_{m3} instead of cancellation. In this work, S values reported in the literature for experimental devices were considered.

After the device-level engineering of MMG, compact models of the devices are done using MVSG model **[10]**, shown in Fig. 2(i)-(j). One tone load pull simulation at 5 GHz shows that the gain of the MMG HEMT is more linear than a conventional HEMT ($P_{1\text{-dB}}$ = 0.59 W/mm, 3.64 W/mm for conventional HEMT and MMG with S = 0.43 FLP factor respectively) for a longer portion of input RF power, as depicted in Fig. 3(a). Furthermore, the PAE of MMG HEMT, considering strong FLP (S = 0.43), is higher in the linear operating region compared to conventional HEMT. Two-tone load-pull simulation was conducted to evaluate RF linearity. The center frequency was set at 5 GHz with a frequency spacing of 10 MHz. The DC quiescent bias point was chosen at $V_{DS,Q}$ = 28 V, $I_{D,Q}$ = {50, 73, 90, 105} mA/mm – all four corresponding to deep Class AB operation. As illustrated in Fig. 3(b), the third order harmonic (P_{3rd}) output power is considerably lower in case of MMG, validating its capability to suppress non-linear higher order power components. The slope of P_{3rd} in case of MMG is appreciably minimized.

The output-referred third-order intercept (OIP3) for planar and MMG HEMT is shown in Fig. 4(a). The linearity metrics are extracted at P_{out} = 15 dBm as in **[6]**. The sweet spot for MMG HEMT shifts to lower $I_{D,Q}$ (50 mA/mm, deeper Class AB) with S = 0.43 when compared to no pinning considered (mid-level $I_{D,Q}$ = 73 mA/mm). The improvement in OIP3 is eventually better in case of pinning factor S = 0.43, supporting the device level optimization achieved. Improvement in OIP3 is 2.2 dB, 7.9 dB and 10.8 dB for S = 1, 0.70 and 0.43 respectively compared to planar HEMT, at $I_{D,Q}$ = 50 mA/mm. OIP3/P_{dc} is found the highest (18.9 dB) for S = 0.43, as shown in Fig. 4(b). Third order intermodulation distortion (IMD3) for the proposed architecture also outcasts the planar HEMT at all pinning conditions as shown in Fig. 4(c). The IMD3 is distinctly lower for MMG schemes. Especially considering FLP factor S = 0.43, IMD3 is lower by ~32dB in a considerable output power range (15–25 dBm) compared to conventional HEMT, as shown in Fig. 4(d).

In GaN HEMT PAs, to maintain a desired level of IMD3, output power back-off (OBO) is a system-level requirement for PA operation, at the expense of PAE. This simulation demonstrates that the required IMD3 can be obtained at lower OBO even if the FLP is included in the simulation framework. Fig. 5(a) shows the achieved IMD3 at three OBOs. It is remarkable that, even after considering practical FLP, a lower IMD3 value can be achieved, manifesting the viability of highly linear operation of the MMG HEMT (13.9 dB lower than conventional HEMT at 6 dB OBO with S = 0.43). The PAE *vs.* OBO trend demonstrated in Fig. 5(b) confirms that, PAE is not compromised for linear operation of PAs (37.2 % for MMG, 31.4 % for conventional HEMT, at 6 dB OBO, S = 0.43). At 6 dB OBO, a consequent lower IMD3 and higher PAE relieve the linearity-efficiency trade-off. Fig. 6(a) shows delayed gain compression ($P_{1\text{-dB}}$ is 3.0 W/mm higher in MMG with FLP factor, S = 0.43; compared to conventional HEMT) for MMG HEMT validating MMG HEMT's capability to operate linearly at higher output power even with finite FLP factors. Though P_{sat} value is 1.6 W/mm lower in MMG [Fig. 6(b)] with strong FLP (S = 0.43) than conventional HEMT, a high-power linear operation is only feasible in MMG.

Conclusion

The influence of FLP in Schottky gate region on the transistor's RF linearity, with reference to MMG HEMT, is systematically investigated. MMG architecture is an effective approach to enhance GaN HEMT linearity by modulating the V_t and hence, suppress g_{m3}. However, for a detailed and practical analysis, FLP should be duly considered. Analysis of MMG in the presence of FLP considering two experimental values of S reveals that, device-level g_{m3} suppression, and consequently large-signal linearity metrics, can be improved even in the presence of FLP. In the broader context, this work offers insights into the "FLP-robustness" of unique transistor architectures, as exemplified by the novel MMG HEMT, to deliver higher RF linearity.

Acknowledgements: This work was supported in part by the Bangladesh University of Engineering and Technology, and in part by the Air Force Office of Scientific Research (AFOSR) under Grant No. FA9550-22-1-0367.

References

[1] E. Zanoni *et al.* "Microwave and Millimeter-Wave GaN HEMTs: Impact of Epitaxial Structure on Short-Channel Effects, Electron Trapping, and Reliability," *IEEE Trans. Electron Devices* (2023).

[2] K. H. Teo, *et al*. "Emerging GaN technologies for power, RF, digital, and quantum computing applications: Recent advances and prospects" *J. Appl. Phys.*130.16 (2021).

[3] J. -S. Moon *et al.* "High-Speed Graded-Channel GaN HEMTs with Linearity and Efficiency" 2020 *IEEE/MTT-S International Microwave Symposium (IMS)*, 2020, pp. 573-575.

[4] F. Zhang *et al*. "Linearity Enhancement of AlGaN/GaN HEMTs with Selective-Area Charge Implantation" *IEEE Electron Device Lett*., vol. 43, Nov. 2022.

[5] V. M. Bermudez. "Simple interpretation of metal/wurtzite–GaN barrier heights" *J. Appl. Phys.* 15 July 1999; 86 (2): 1170–1171.

[6] M. T. Azad *et al*. "AlGaN/GaN-Based Multimetal Gated High-Electron-Mobility Transistor With Improved Linearity" *IEEE Trans. Electron Devices* 70.11 (2023): 5570-5576

[7] Q. Xie *et al*. "Towards DTCO in High Temperature GaN-on-Si Technology: Arithmetic Logic Unit at 300 °C and CAD Framework up to 500 °C" *2023 IEEE Symp. VLSI Technol. Circuits (VLSI Technol. Circuits)*, Jun. 2023.

[8] N. Chowdhury *et al*. "Performance Estimation of GaN CMOS Technology" *2021 Device Research Conference (DRC)*, Santa Barbara, CA, USA, 2021, pp. 1-2.

[9] G. Fisichella *et al*. "Current transport in graphene/AlGaN/GaN vertical heterostructures probed at nanoscale" *Nanoscale* 6.15 (2014): 8671-8680.

[10] R. Fang *et al.* "MVSG GaN-HEMT Model: Approach to Simulate Fringing Field Capacitances, Gate Current De-biasing, and Charge Trapping Effects," *2022 IEEE BiCMOS and Compound Semiconductor Integrated Circuits and Technology Symposium (BCICTS)*, 2022, pp. 21-24.

Multimetal Gated Device Architecture and Methodology

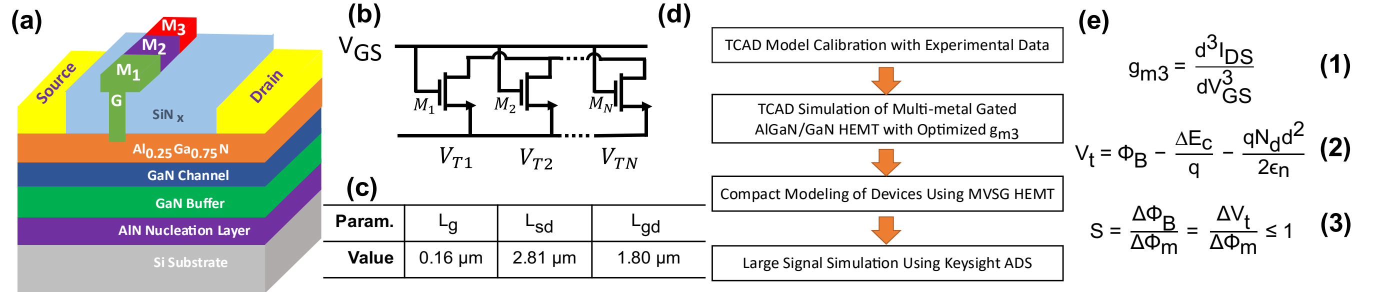

Fig. 1: (a) 3-D schematic of the Multimetal gated AlGaN/GaN HEMT. M_1, M_2, & M_3 are different metals with their numbers, widths, and work functions as optimization parameters. (b) Circuit visualization of the MMG technique. MMG HEMT follows the principle of parallel connected HEMTs with distinct threshold voltage V_{T1}, V_{T2}, V_{TN}. (c) Structural parameters of the proposed device. (d) Methodology of this work, including the TCAD model calibration and simulation, compact modeling, and large-signal circuit simulation, in the specified order. (d) Definitions of g_{m3}, V_t and S.

Third Order Transconductance Improvement considering Fermi Level Pinning (FLP)

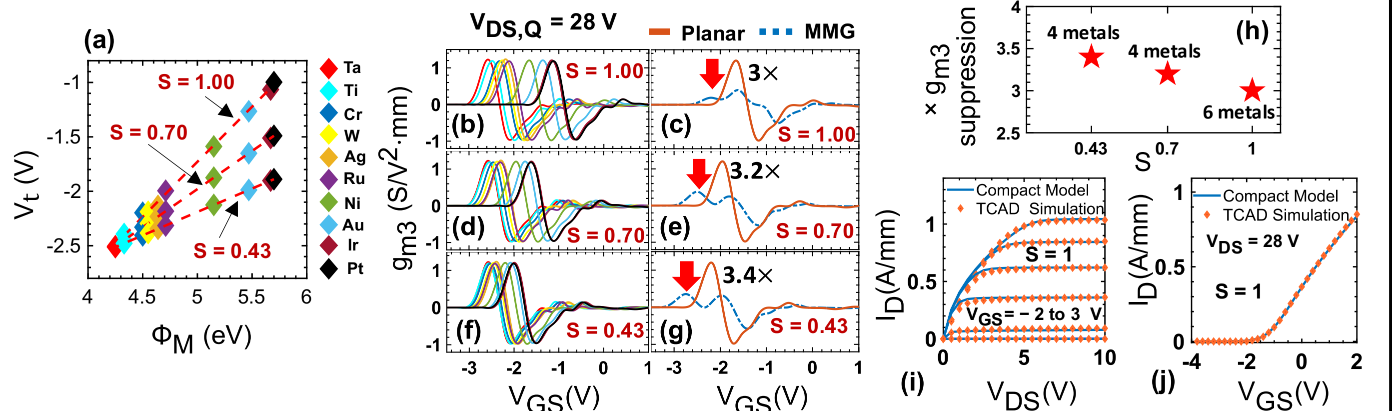

Fig. 2: (a) Threshold variation with gate-metal work-functions for different Fermi-Level pinning factors, *S*. A linear relation is preserved even though the standard deviations of V_t values decrease with decreasing *S*. (b), (d) and (f) g_{m3} peaks of different metals gets closer as the pinning effect takes charge. (c), (e) and (g) Optimization of g_{m3} with Fermi level pinning effect considered. (h) Magnitude of reduction in g_{m3} *vs.* FLP factor, *S*. Number of metals required is mentioned alongside. (i)-(j) Compact Modeling of the MMG HEMT using MVSG model showing I_D-V_{DS} and I_D-V_{GS} characteristics of MMG HEMT.

RF Large Signal Performance considering FLP in MMG HEMT

Solid Line – Conv. Dotted line – MMG (S=0.43) ● Planar ▶ S = 1.00 ◆ S = 0.70 ★ S = 0.43

Fig. 3: (a) Fundamental output power, gain and PAE *vs.* input RF power for Conventional and MMG HEMT. Gain curve showing delayed compression in MMG for FLP factor, *S* = 0.43 ($V_{DS,Q}$ = 28 V, $I_{D,Q}$ = 50 mA/mm, *f* = 5 GHz) (b) Fundamental and Third Harmonic Power *vs.* input RF power. Lower P_{3rd} for the MMG HEMT compared to Conventional HEMT showing better harmonic suppression even in the presence of FLP. (*f* = 5 GHz, Δ*f* = 10 MHz) In this work, device width is 100 µm.

Fig. 4: (a) OIP3 (b) OIP3/P_{dc} (c) IMD3 at different current bias condition shows MMG HEMT outstands conventional HEMT at three FLPs. The data are extracted at 15 dBm output power. The best operating bias is circled in the figures. (d) IMD3 at a range of output power showing better harmonic suppression capability of MMG up to higher output powers.

Fig. 5: (a) Improved (suppressed) IMD3 achieved for MMG (for all finite FLPs) at lower OBO suggesting its viability as an effective device to operating close to P_{sat}. (b) PAE at different output power back-off (OBO) for conventional HEMT and MMG HEMT considering three FLP factors. ($V_{DS,Q}$ = 28 V, $I_{D,Q}$ = 50 mA/mm)

Fig.6: Impact of FLP on (a) output referred 1-dB compression point and (b) P_{sat}. The results reflect MMG HEMT's capability to operate linearly at higher output power even with finite FLP factors.